Alteration of *O*-GlcNAcylation affects serine phosphorylation and regulates gene expression and activity of pyruvate kinase M2 in colorectal cancer cells

PARUNYA CHAIYAWAT[1], DARANEE CHOKCHAICHAMNANKIT[2], KRIENGSAK LIRDPRAPAMONGKOL[1,2], CHANTRAGAN SRISOMSAP[1,2], JISNUSON SVASTI[1,2] and VORARATT CHAMPATTANACHAI[1,2]

[1]Applied Biological Sciences Program, Chulabhorn Graduate Institute, Bangkok; [2]Laboratory of Biochemistry, Chulabhorn Research Institute, Bangkok, Thailand

Received May 11, 2015; Accepted July 27, 2015

DOI: 10.3892/or.2015.4178

Abstract. *O*-GlcNAcylation is a dynamic post-translational modification that has extensive crosstalk with phosphorylation either at the same or adjacent sites of various proteins. We have previously reported that *O*-GlcNAcylation level was increased in primary breast and colorectal cancer, but the interplay of the two modifications remains unclear. Therefore, we explored crosstalk of the modifications by RNA interference against *O*-GlcNAc transferase (OGT) in colorectal cancer cells. Two-dimensional immunoblotting and mass spectrometric analysis showed that the levels of *O*-GlcNAc and serine phosphorylation of many proteins including serine hydroxymethyltransferase, cytokeratin-8, pyruvate kinase M2 (PKM2), heterogeneous nuclear ribonucleoprotein L, and lamin-B1, were reduced in siOGT cells compared to siScramble cells. In HT29 cells, immunoprecipitated PKM2 revealed decreased *O*-GlcNAc and serine phosphorylation levels after siOGT knockdown, but increased levels after treatment with Thiamet-G, an inhibitor of *O*-GlcNAcase (OGA). In addition, when global *O*-GlcNAcylation was enhanced by treating cells with Thiamet-G, PKM2 expression level was upregulated, but PKM2-specific activity was decreased. On the other hand, in OGT knockdown cells, PKM2 expression level was downregulated, but PKM2-specific activity was increased. Moreover, the metastatic colorectal cancer cells, SW620, had more *O*-GlcNAc-PKM2 and showed lower PKM2-specific activity compared to the non-metastatic colorectal cancer SW480 cells. These results suggested roles of *O*-GlcNAcylation in modulating serine phosphorylation, as well as in regulating PKM2 activity and expression. Interfering levels of *O*-GlcNAcylation of PKM2 may be a novel target in controlling cancer metabolism and tumorigenesis of colorectal cancer.

Correspondence to: Dr Voraratt Champattanachai, Laboratory of Biochemistry, Chulabhorn Research Institute, 54 Kamphaeng Phet 6, Laksi, Bangkok 10210, Thailand
E-mail: voraratt@cri.or.th

Abbreviations: 2DE, two-dimensional gel electrophoresis; CaMKIV, Ca^{2+}/calmodulin-dependent protein kinase IV; CK8, cytokeratin-8 or keratin-8; FBP, fructose 1,6-bisphosphate; G6P, glucose-6-phosphate; HBP, hexosamine biosynthesis pathway; HNRNPL, heterogeneous nuclear ribonucleoprotein L; IEF, isoelectric focusing; LB1, lamin-B1; *O*-GlcNAc, *O*-linked *N*-acetyl-D-glucosamine; OGA, *O*-GlcNAcase; OGT, *O*-GlcNAc transferase; PEP, phosphoenolpyruvate; PK, pyruvate kinase; PKCδ, protein kinase C δ; PKM2, pyruvate kinase M2; SHMT, serine hydroxymethyltransferase; TMG, Thiamet-G; UDP-GlcNAc, uridine diphospho-*N*-acetylglucosamine

Key words: colorectal cancer, hexosamine biosynthesis pathway, *O*-GlcNAcylation, phosphorylation, pyruvate kinase M2

Introduction

Cancer cells utilize glucose at a high rate to support their rapid proliferation and biosynthesis, and this occurs via glycolysis rather than metabolizing pyruvate through oxidative phosphorylation in the TCA cycle (1). Pyruvate kinase (PK) is a key rate-limiting enzyme in the glycolytic pathway and has a well-defined role in the Warburg effect (2,3). Pyruvate kinase catalyzes the transfer of a phosphate group from phosphoenolpyruvate (PEP) to ADP producing ATP and pyruvate (1). Two genes encode for four isoforms of pyruvate kinase that are specifically expressed in different tissues. PKL and PKR isoforms are encoded by the *PKLR* gene, while PKM1 and pyruvate kinase M2 (PKM2) are encoded by *PKM* gene. By alternative splicing, PKM2 carries exon 10, but not exon 9 as found in PKM1 (4). PKM2 exists in three forms including an inactive monomer, a low activity dimer, and a high activity tetramer. In cancer cells, a dominant form of PKM2 is the dimer conformation, which paradoxically leads to a high lactate production as in the Warburg effect (5). Highly proliferating cancer cells require building blocks for the synthesis of lipids, nucleotides and amino acids. Decreased PKM2 activity will slow glycolysis rate enabling cancer cells to produce macromolecule precursors from glycolytic intermediates, such as glucose-6-phosphate (G6P) through the pentose phosphate pathway (PPP) and the hexosamine biosynthesis pathway (HBP) (2,3,6).

O-GlcNAcylation is a discrete glycosylation in which target proteins are modified at the hydroxyl group of serine and/or threonine by one molecule of *N*-acetyl-D-glucosamine (*O*-GlcNAc) (7). This glycosylation may take place in the cytoplasm, nucleus, and mitochondria. Two key enzymes, *O*-GlcNAc transferase (OGT) and *O*-GlcNAcase (OGA) regulate *O*-GlcNAcylation by catalyzing the addition and removal of an *O*-GlcNAc group from proteins, respectively. Enzymatic activity of OGT is sensitive to the concentration of its donor substrate; uridine diphospho-*N*-acetylglucosamine (UDP-GlcNAc) (8). UDP-GlcNAc is the end product of the HBP and is built up from a variety of nutrients including glucose, glutamine, fatty acids (acetyl) and uridine (7,9). Cancer cells can take up both glucose and glutamine more than normal cells (10). Increasing flux of glucose and glutamine through the HBP leads to increased *O*-GlcNAcylation. Enhanced level of *O*-GlcNAcylation is observed in most cancers including colorectal cancer (11,12).

Growing evidence reveals that *O*-GlcNAcylation has extensive crosstalk with phosphorylation either on the same or adjacent sites of various proteins (13). At first glance, interplay between *O*-GlcNAcylation and *O*-phosphorylation is proposed as a Yin-Yang model with a shared modification site in which *O*-GlcNAc on/off cycle is rapidly regulated in similar time scale and cellular state as phosphorylation (13). Effects in several proteins are reciprocal, while others are not (14). The interplay of these two post-translational protein modifications can work simultaneously and regulate protein function, stabilization, translocation, complex formation and enzyme activity, subsequently affecting cellular signaling pathways.

Previously, we showed that the levels of *O*-GlcNAcylation and OGT were increased in primary breast and colorectal cancer tissues and many proteins were selectively modified by *O*-GlcNAc in both cancers (12,15). In this study, we explored the interplay of *O*-GlcNAcylation and phosphorylation by knocking down *OGT* gene in colorectal cancer cell lines. Using a combination of proteomic approaches, two-dimensional gel electrophoresis (2DE), *O*-GlcNAc and serine phosphorylation immunoblotting, followed with LC-MS/MS analysis, we identified a number of proteins associated with aberrant *O*-GlcNAcylation and phosphorylation. In addition, by using siOGT and OGA inhibitor approaches, we demonstrated that reduction of *O*-GlcNAc led to decreased phosphorylation of PKM2 whereas increasing *O*-GlcNAc gave the opposite results. Furthermore, pyruvate kinase activity as well as expression levels of PKM2 were modulated in response to alterations of global *O*-GlcNAcylation levels in colorectal cancer cell lines.

Materials and methods

Cell culture, Thiamet-G, and siRNA transfection. Cell culture medium and supplementary products were purchased from Invitrogen. Normal colon epithelial cell, CCD841 CoN (ATCC; American Type Culture Collection) was a gift from Dr Jutamaad Satayavivad, Chulabhorn Research Institute, Thailand. CCD841 CoN cells were cultured in Dulbecco's modified Eagle's medium (DMEM) with high glucose and pyruvate supplemented with 10% FBS and 1% L-glutamine. The human colorectal cancer cell lines, HT29, SW480 and SW620 were purchased from ATCC. HT29 was cultured in DMEM supplemented with 10% FBS. SW480 and SW620 were maintained in RPMI-1640 medium supplemented with 10% FBS. All the cells were supplemented with 1% penicillin/streptomycin and maintained at 37˚C in humidified 5% CO_2 incubator. HT29 cells were treated with Thiamet-G (TMG; Sigma), an inhibitor of OGA at 10 μM for 48 h. Stealth siRNA targeting *OGT* gene was as follows: sense, 5'-UAAUCAUUUCAAUAA CUGCUUCUGC-3' and antisense, 5'-GCAGAAGCAGUUA UUGAAAUGAUUA-3' (Invitrogen). Stealth scrambled siRNA medium GC duplex (Invitrogen) was used as a negative control. To transiently knockdown OGT, stealth siOGT or scrambled siRNA (control) was transfected to HT29 cells for 72 h using Lipofectamine™ 2000 (Invitrogen) according to manufacturer's protocol.

Antibodies. Antibodies for *O*-GlcNAc, OGA, polyclonal PKM2 antibody were purchased from Abcam. Antibody for OGT was purchased from Sigma. Monoclonal antibody for PKM2 was purchased from Santa Cruz Biotechnology. Antibodies for phosphoserine and phosphothreonine were purchased from Qiagen.

Preparation of cell lysates and western blot analysis. Cell lysate extraction was prepared in RIPA buffer as previously described (15). Protein concentration was determined using Bradford assay. Extracted proteins (10-30 μg) were separated in 10% SDS-PAGE and transferred to PVDF membranes (Millipore). Blots were probed with indicated antibodies. Bands on immunoblots were detected using WesternBright ECL (Advansta) and chemiluminescent signals images were captured using ImageQuant™ LAS 4000 digital imaging system (GE Healthcare).

Two-dimensional gel electrophoresis and western blot analysis. For two-dimensional isoelectric focusing (IEF) and polyacrylamide gel electrophoresis (2D-IEF/PAGE), cells were lysed in 2D lysis buffer and extracted proteins (100-150 μg) were separated by IEF using Immobiline Drystrips (7 cm, pH 3-10, non-linear; GE Healthcare). The 2DE was performed as previously described (15). After electrophoresis was finished, proteins in gels were transferred to PVDF membranes. The membranes were stained by SYPRO Ruby (Thermo Scientific) using the manufacturer's recommendations and the signals were scanned using Ettan DIGE Imager (GE Healthcare) prior to probing with *O*-GlcNAc and phosphoserine antibodies. In order to normalize the *O*-GlcNAc and phosphoserine-modified protein spots with SYPRO Ruby protein staining on 2DE, proteins extracted from siOGT and siScramble cells were loaded equally. The exposure times on Ettan DIGE Imager and chemiluminescence were exactly the same.

In-gel digestion. Protein spots, in which phosphoserine levels were altered in siOGT-knockdown HT29 cells and consistently observed in three independent 2DE experiments, were excised and subjected to in-gel trypsin digestion as previously described (16). Briefly, excised gels were destained with 50% ACN in 0.1 M NH_4HCO_3, reduced with 10 mM DTT, alkylated in 100 mM iodoacetamide and digested with trypsin (Promega) at 37˚C overnight. The digested peptides were dried and collected for protein identification by LC-MS/MS.

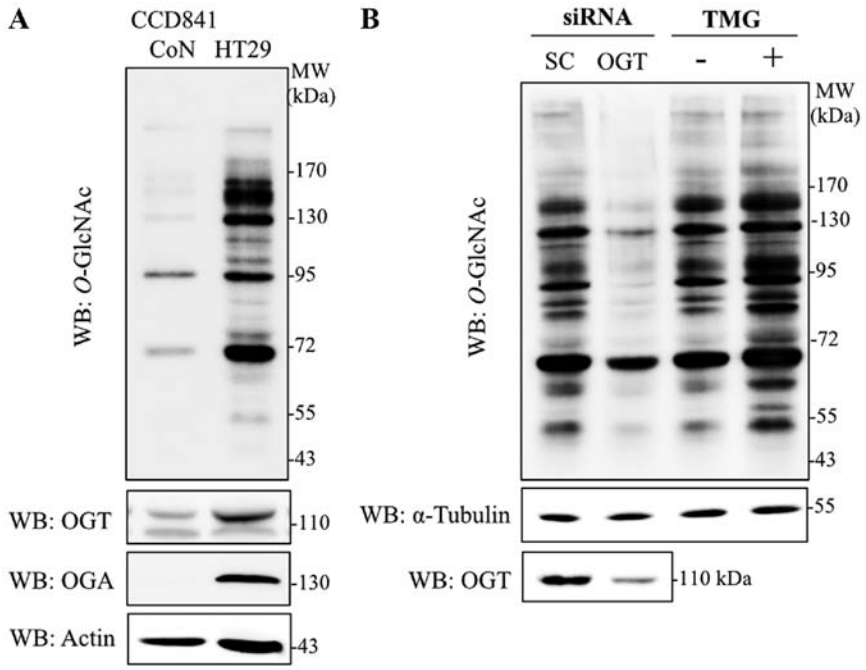

Figure 1. Alteration of *O*-GlcNAcylation, OGT and OGA levels in HT29. (A) Immunoblots of *O*-GlcNAc, OGT and OGA in HT29 colorectal cancer cells compared to CCD841 CoN, normal colon epithelial cell. (B) Immunoblots of *O*-GlcNAc and OGT of siScramble compared to siOGT-transfected HT29 cells (72 h) as well as untreated and 10 μM TMG-treated cells (48 h). OGT, *O*-GlcNAc transferase; OGA, *O*-GlcNAcase; TMG, Thiamet-G.

Protein identification by LC-MS/MS. The digested peptides were identified using Nanoflow liquid chromatography coupled with the amaZon speed ion trap mass spectrometry (Bruker, USA) as previously described (17). Protein identification was performed using Mascot search engine with NCBInr version 20130630 sequence databases (http://www.matrixscience.com). Search parameters were set as follows: peptide mass tolerance was 1.2 Da, MS/MS ion mass tolerance was 0.6 Da, allowance was set to 1 missed cleavage, enzyme set as trypsin, the limit of peptide charges was 1^+, 2^+, and 3^+. Proteins with molecular weight and p*I* consistent to spot on 2DE gel were considered positively identified.

Pyruvate kinase activity assay. The pyruvate kinase activity of cell lysates (5 μg) of HT29, SW480 and SW620 was determined according to the manufacturer's protocol (BioVision). One unit of pyruvate kinase is the amount of enzyme that transfers a phosphate group from PEP to ADP, yielding 1.0 μmol of pyruvate/min at 25˚C. The specific activity of PKM2 was calculated using the pyruvate kinase activity divided by the protein amount of PKM2 (immunoblot intensity).

Immunoprecipitation. Whole cell lysate (500 μg) was incubated with 3 μg of polyclonal PKM2 antibody with gentle end-over-end mixing overnight at 4˚C. The antibody-sample complex was incubated with 20 μl of protein A/G agarose resin (Thermo Scientific) with gentle end-over-end mixing for 2 h at 4˚C. Unbound fraction was discarded by centrifugation at 1,000 x g for 1 min. The agarose resin was washed with TBS buffer three times and boiled in 2X SDS sample buffer for 10 min. Eluent was collected by centrifugation for 5 min at 1,000 x g.

Real-time RT-PCR. RNA was extracted from HT29 cells using RNeasy Mini kit (Qiagen) following the manufacturer's instructions. To synthesize first-strand cDNA, reverse transcription of 2 μg of total RNA was catalyzed by SuperScript™ III Reverse Transcriptase (Invitrogen). The primers used are PKM2 forward, GAG GCC TCC TTC AAG TGC T and reverse, CCA GAC TTG GTG AGG ACG AT; and PKM1 forward, ACC GCA AGC TGT TTG AAG AA and reverse, TCC ATG AGG TCT GTG GAG TG. Real-time PCR was performed in StepOnePlus™ Real-Time PCR system (Applied Biosystems) using KAPA SYBR®FAST qPCR kits (Kapa Biosystems). To compare the relative mRNA expression of each treatment, 18S rRNA was used as an internal control. The thermal profile was set as follows: an initial incubation step at 95˚C for 15 min, followed by 40 cycles of denaturation at 95˚C for 15 sec, annealing at 65˚C for 30 sec, and extension at 72˚C for 30 sec, respectively. Mean threshold cycle (CT) was calculated from triplicates. Data were analyzed using $2^{-\Delta Ct}$ method as previously described (18).

Statistical analysis. The statistical analysis was analyzed using unpaired Student's t-test to test for the difference between two groups. The statistical significance was defined at $p \leq 0.05$.

Results

Alteration of O-GlcNAcylation, OGT and OGA levels in colorectal cancer cells. Immunoblotting with antibodies specific to *O*-GlcNAc (RL2), OGT and OGA were used to determine the levels of global *O*-GlcNAcylation, and *O*-GlcNAc cycling enzymes in colorectal cancer cells, respectively. *O*-GlcNAcylation, OGT and OGA levels were obviously increased in HT29 cells in comparison to normal colon epithelia cells, CCD841 CoN (Fig. 1A). As OGT catalyzes an addition of *O*-GlcNAc on target proteins observed in various cancers, OGT transient-knockdown HT29 cells were

Table I. The identified serine-phosphorylated-modified proteins in HT29 cells.

Spot no.	Accession nos.	Protein names	MW/PI (kDa/p*I*)	Peptide matches	Coverage (%)	Scores	Volume of phosphoserine[a] SC	Volume of phosphoserine[a] siOGT	Fold-changes[b]	Reports for *O*-GlcNAcylation
1	gil19923315	Serine hydroxymethyl-transferase, mitochondrial	56414/8.76	38	45	489	3.49	0.903	-3.86	N/A
2	gil181573	Cytokeratin-8	53529/5.52	19	33	623	15.9	11.2	-1.42	Chou *et al* (28)
3	gil189998	M2-type pyruvate kinase	58447/7.95	19	37	440	6.29	2.16	-2.91	Champattanachai *et al* (15)
4	gil119577231	Heterogeneous nuclear ribonucleo-protein L	64720/8.46	16	21	160	2.09	1.11	-1.88	N/A
5	gil5031877	Lamin-B1 isoform 1	66653/5.11	36	38	537	2.82	1.54	-1.83	N/A

[a]Volume of phosphoserine from immunoblots measured by Master 2D Platinum software; [b]ratio of phosphoserine volume in siOGT-knockdown relative to scramble-treated HT29 cells; SC means scramble-treated HT29 cells; minus sign (-) denotes decreased phosphoserine level in siOGT-knockdown HT29 cells; N/A means not available; OGT, O-GlcNAc transferase.

established. Transfection of siOGT remarkably reduced OGT and *O*-GlcNAcylation levels when compared to siScramble control (Fig. 1B). Furthermore, when a potent OGA inhibitor, TMG, was used to decrease removal of the *O*-GlcNAc molecule, global *O*-GlcNAcylation was enhanced. *O*-GlcNAc level was clearly elevated in HT29 cells treated with TMG (Fig. 1B).

Interplay of O-GlcNAcylation and phosphorylation in response to OGT transient-knockdown. Since *O*-GlcNAcylation is selective for serine and/or threonine residues, changes in global *O*-GlcNAcylation may influence the phosphorylation of various proteins. To demonstrate an association between *O*-GlcNAcylation and *O*-phosphorylation in colorectal cancer cells, 2DE was performed on proteins isolated from OGT-knockdown and scrambled siRNA-transfected HT29 cells, followed by immunoblotting with antibodies specific to *O*-GlcNAc and phosphoserine. 2DE immunoblots of siOGT-knockdown showed decreased *O*-GlcNAcylation of various proteins compared to siScramble-transfected cells (Fig. 2A). Interestingly, siOGT-knockdown resulted in reduction of serine phosphorylation compared to scramble control cells (Fig. 2B). *O*-GlcNAc and phosphoserine immunoblots were aligned to SYPRO Ruby staining blots and five protein spots were clearly matched to the spots on immunoblots (Fig. 2C). *O*-GlcNAc and serine phosphorylation levels of five protein spots (spot no. 1-5) were decreased or undetectable in siOGT-treated cells, when compared to scramble control cells (Fig. 2D and E). These phosphorylated protein spots were cut, digested with trypsin and subjected to LC-MS/MS. Five proteins were identified and observed in three independent experiments, as shown in Table I. Serine phosphorylation levels of serine hydroxymethyltransferase (SHMT) (spot no. 1), cytokeratin-8 (spot no. 2), heterogeneous nuclear ribonucleoprotein L (HNRNPL) (spot no. 4), and lamin-B1 (spot no. 5) were decreased in siOGT-knockdown cells (Fig. 2B and E). Four spots (spot no. 1-4) showed *O*-GlcNAc modification on *O*-GlcNAc-2DE blots whereas *O*-GlcNAc modification of lamin-B1 (spot no. 5) was not observed in either scrambled or siOGT-knockdown HT29 cells (Fig. 2A and D). Notably, PKM2 (spot no. 3) showed a remarkable reduction of *O*-GlcNAc as well as serine phosphorylation in siOGT-knockdown HT29 cells but not in threonine-phosphorylation (data not shown).

Association between O-GlcNAcylation and serine phosphorylation of PKM2. According to the results from 2DE, PKM2 was *O*-GlcNAcylated in HT29 cells, but the level of *O*-GlcNAc was reduced in cells with siOGT knocked down. To confirm whether PKM2 is *O*-GlcNAcylated, PKM2 from controls, siOGT-knockdown and TMG-treated HT29 cell lysates were immunoprecipitated, separated on SDS-PAGE and probed with antibody specific to *O*-GlcNAc. The results showed that *O*-GlcNAcylation of PKM2 was reduced in siOGT-knockdown cells but increased in TMG-treated cells (Fig. 3A and B). We further verified an association between *O*-GlcNAcylation and phosphorylation of pulled down PKM2. After siOGT knockdown, decreased *O*-GlcNAcylation resulted in lower *O*-GlcNAcylated and serine phosphorylated PKM2, while upon treatment with TMG, increased *O*-GlcNAcylation significantly enhanced serine phosphorylation of PKM2 (Fig. 3A and B).

O-GlcNAc sites of PKM2 were computationally predicted using two available websites including YinOYang and *O*-GlcNAcScan (http://www. cbs.dtu.dk/services/YinOYang/ and http://cbsb.lombardi.georgetown.edu/hulab/OGAP.html). The combination of *O*-GlcNAc sites from the two programs are shown in Fig. 3C. YinOYang predicted seven *O*-GlcNAc sites, which are Ser2, Ser6, Ser222, Thr405, Ser406, Thr454 and Thr459, while *O*-GlcNAcScan also predicted seven sites including Ser6, Ser55, Ser67, Thr143, Ser249, Ser406

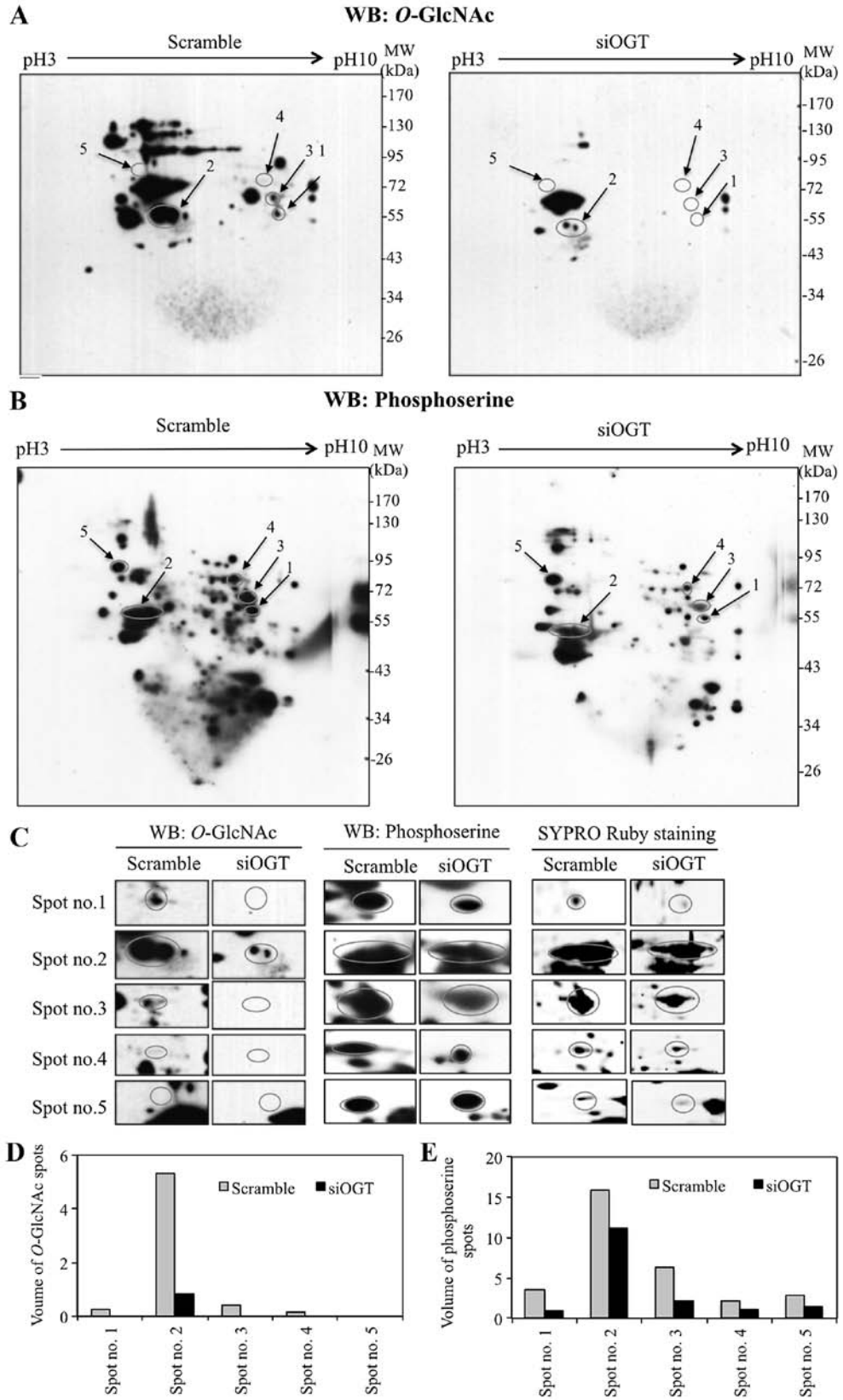

Figure 2. Representative 2DE immunoblots of *O*-GlcNAcylated and serine phosphorylated proteins of scrambled and siOGT-knockdown HT29 cells. Five spots in siOGT-knockdown group showed significantly reduction in (A) *O*-GlcNAc and (B) serine phosphorylation detected by immunoblotting. (C) Zoom-in views of individual *O*-GlcNAc, phosphoserine, and SYPRO Ruby protein spots in scrambled and siOGT-knockdown cells. The bar graphs show the volume of (D) *O*-GlcNAc and (E) phosphoserine of protein spot no. 1-5 observed in siOGT-knockdown and siScramble cells measured by ImageMaster 2D Platinum version 7.0. Arrows indicate protein spots identified by LC-MS/MS. 2DE, two-dimensional gel electrophoresis; OGT, *O*-GlcNAc transferase.

and Thr454. Shared possible *O*-GlcNAc sites from the two programs are Ser6, Ser222, Ser406 and Thr454. Together, eleven *O*-GlcNAc-modified sites were predicted and found in various parts throughout the PKM2 structure. Serine

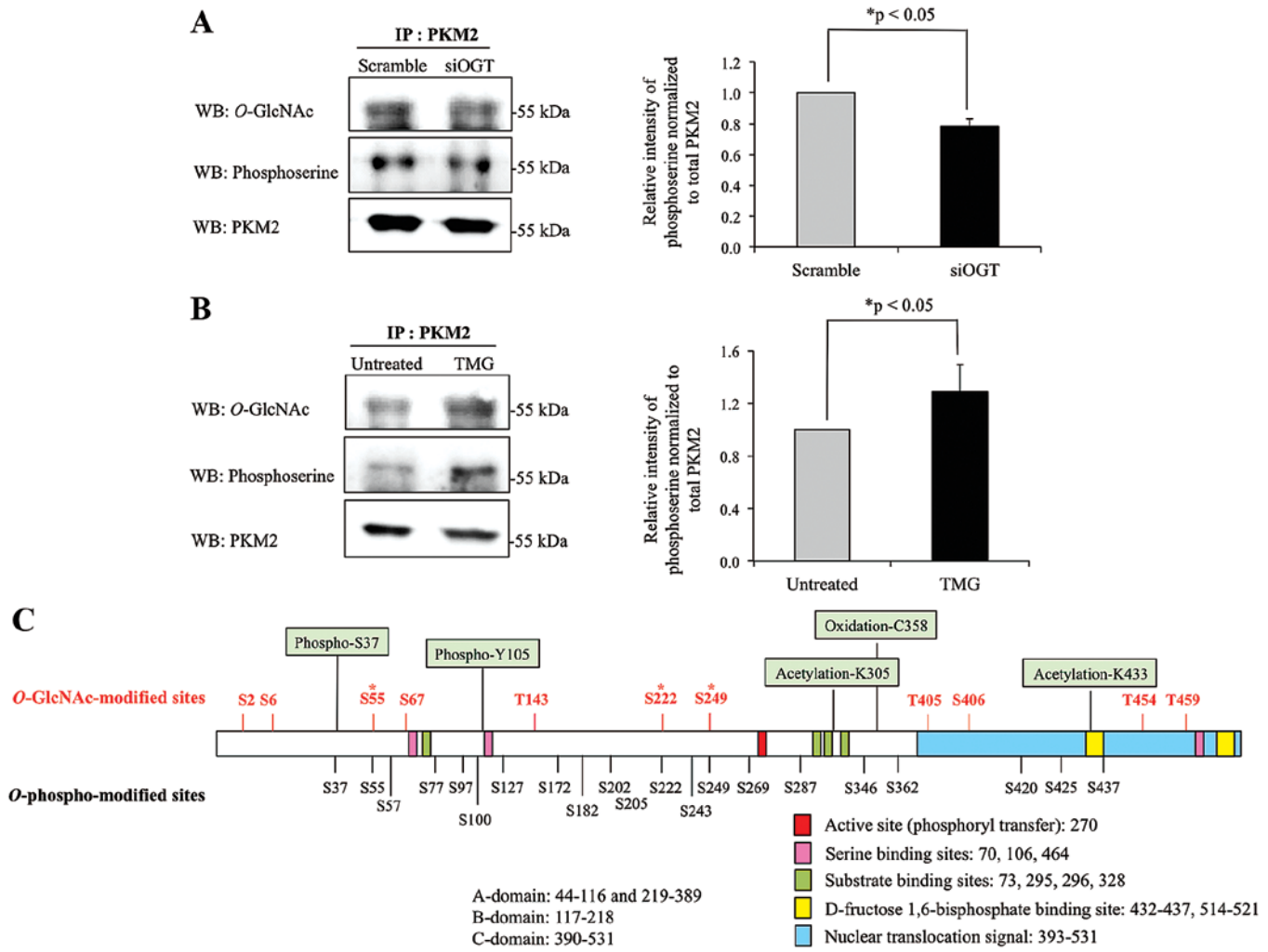

Figure 3. Confirmation of altered *O*-GlcNAcylation and serine phosphorylation levels of PKM2 in siOGT-knockdown and TMG-treated HT29 cells. Immunoprecipitated PKM2 from total whole cell lysates was separated in SDS-PAGE and immunoblotted with specific antibodies to *O*-GlcNAcylation and serine phosphorylation. Immunoblots of *O*-GlcNAc and serine phosphorylation of pulled down PKM2 from (A) scrambled and siOGT knockdown as well as (B) untreated and TMG-treated HT29 cells. Densitometric analysis shows intensity of serine phosphorylated PKM2 measured by ImageQuant TL program. Data are presented as means ± SD from three independent experiments. (C) Scheme of PKM2 protein shows *O*-GlcNAc-modified sites (predicted using YinOYang and *O*-GlcNAcScan programs) and *O*-phospho-modified serine (PhosphoSitePlus database). The asterisks (*) represent for the possible *O*-GlcNAc and *O*-phospho sites that might competitively occupy at the same site (predicted from YinOYang website). Other previously identified post-translational modifications of PKM2 are displayed as text in boxes. OGT, *O*-GlcNAc transferase; PKM2, pyruvate kinase M2; TMG, Thiamet-G.

phosphorylated sites of PKM2 (data from PhosphoSitePlus database) are also shown in Fig. 3C, with only three sites, Ser55, Ser222 and Ser249 having potential to be competitively occupied by *O*-GlcNAc or *O*-phospho modification.

O-GlcNAcylation regulates expression levels and pyruvate kinase activity of PKM2. The mRNA expression levels of PKM1 and PKM2 were determined using real-time RT-PCR, with results showing that PKM2 mRNA expression level was >10-fold higher in comparison to PKM1 mRNA level in HT29 cells (Fig. 4A). This indicated that the expression of PKM2 predominates in cancer cells. To elucidate role of *O*-GlcNAcylation on PKM2 gene expression level, the expression levels of PKM2 gene were determined in siOGT-knockdown HT29 cells, compared to scramble-treated cells, and in TMG-treated cells compared to untreated cells. PKM2 expression level was significantly downregulated in siOGT-knockdown cells but upregulated in TMG-treated cells (Fig. 4A). Consistent with the real-time RT-PCR results, immunoblots of PKM2 showed alteration in expression levels of PKM2, in harmony with levels of *O*-GlcNAcylation of PKM2 (Fig. 4B). In addition, pyruvate kinase (PK) activity of whole cell lysates of siOGT-knockdown and TMG-treated HT29 cells were measured as shown in Fig. 4C. Lower PK activity was observed in both siOGT-knockdown and TMG-treated HT29 cells compared to their controls. However, since global *O*-GlcNAcylation levels regulated expression of PKM2 enzyme, the ratio of PK activity to PKM2 expression levels detected by immunoblotting was calculated as PKM2-specific activity shown in Fig. 4D. PKM2-specific activity was significantly higher in siOGT-knockdown than scramble-treated HT29 cells. However, the opposite result was observed in TMG-treated HT29 cells compared to untreated controls.

Differential level and activity of O-GlcNAc-modified PKM2 in colorectal cancer cell lines originated from primary and metastatic sites. Further study was performed on *O*-GlcNAc

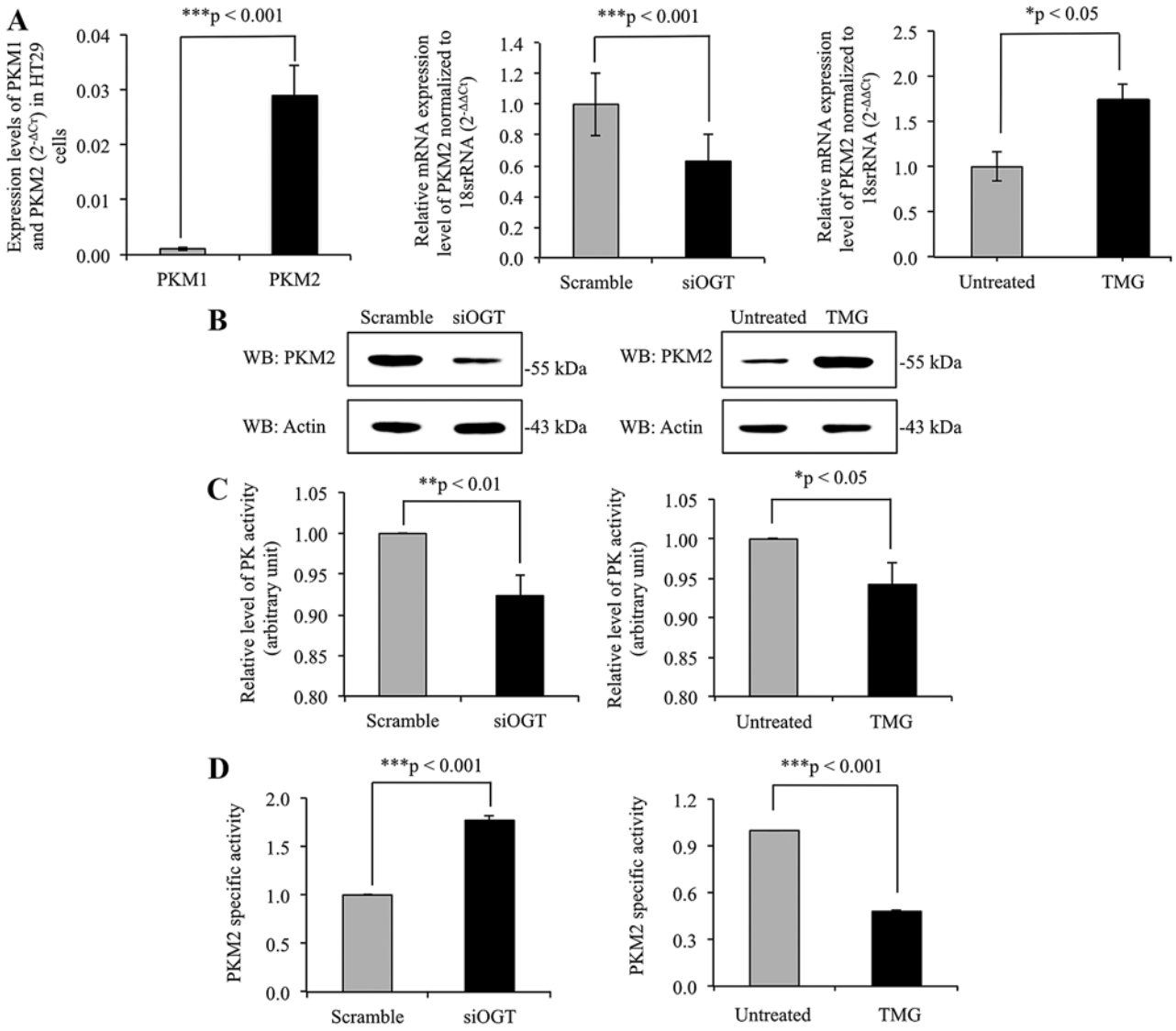

Figure 4. Alterations of expression level and pyruvate kinase activity of PKM2 in siOGT-knockdown and TMG-treated HT29 cells. (A) Real-time RT-PCR of PKM1 and PKM2 expression levels in HT29 cells. PKM2 gene expression levels of siOGT-knockdown and TMG-treated HT29 cells. Data are presented as means ± SD of expression level ($2^{-\Delta Ct}$) and fold-changes ($2^{-\Delta\Delta Ct}$) relative to 18s rRNA from three independent experiments. (B) Immunoblots of PKM2 and actin of siOGT-knockdown and TMG-treated HT29 cells in comparison to their controls (scramble-treated or untreated cells). (C) Relative activity of pyruvate kinase activity in whole cell lysates of scramble-treated and siOGT-knockdown, as well as untreated and TMG-treated HT29 cells. (D) PKM2-specific activity in scramble-treated and siOGT-knockdown, as well as untreated and TMG-treated HT29 cells calculated from relative pyruvate kinase activity (C) normalized to PKM2 expression level detected by immunoblotting (B). Data are presented as means ± SD from three independent experiments. PKM2, pyruvate kinase M2; TMG, Thiamet-G; OGT, *O*-GlcNAc transferase.

modification of PKM2 in primary (non-metastatic) SW480 and metastatic SW620 colorectal cancer cells. Western blotting of whole cell lysates of SW480 and SW620 cells did not show major differences in global *O*-GlcNAcylation, OGT and OGA enzyme levels (Fig. 5A). However, immunoblotting for PKM2 showed that the expression level of PKM2 was significantly enhanced in SW620 cells compared to SW480 cells (Fig. 5B). Assay of PKM2 enzyme activity demonstrated that the SW480 and SW620 cells did not differ significantly (Fig. 5C). However, due to the higher level of PKM2 protein in SW620 cells compared to SW480 cells (Fig. 5B), the specific activity of PKM2 in SW620 appears to be much lower than in SW480 cells (Fig. 5D). To estimate the extent of *O*-GlcNAc modification, PKM2 was immunoprecipitated from whole cell lysates, and interestingly, the level of *O*-GlcNAc modification observed in pulled down PKM2 tended to increase in SW620 cells compared to SW480 cells (Fig. 5E).

Discussion

The increase in *O*-GlcNAcylation in various cancers is well known, and correlates with the increase in glucose and glutamine uptake in cancer cells, which allows cancer cells to utilize available nutrients and accumulate cellular *O*-GlcNAc. Previous study has shown that *O*-GlcNAcylation level was globally increased in colon cancer in comparison to adjacent benign tissues (11,12). Here, we demonstrate that levels of *O*-GlcNAcylation, OGT and OGA were notably increased in the colorectal cancer cell line, HT29, while less change was found in a normal colorectal epithelium cell, CCD841 Con (Fig. 1A).

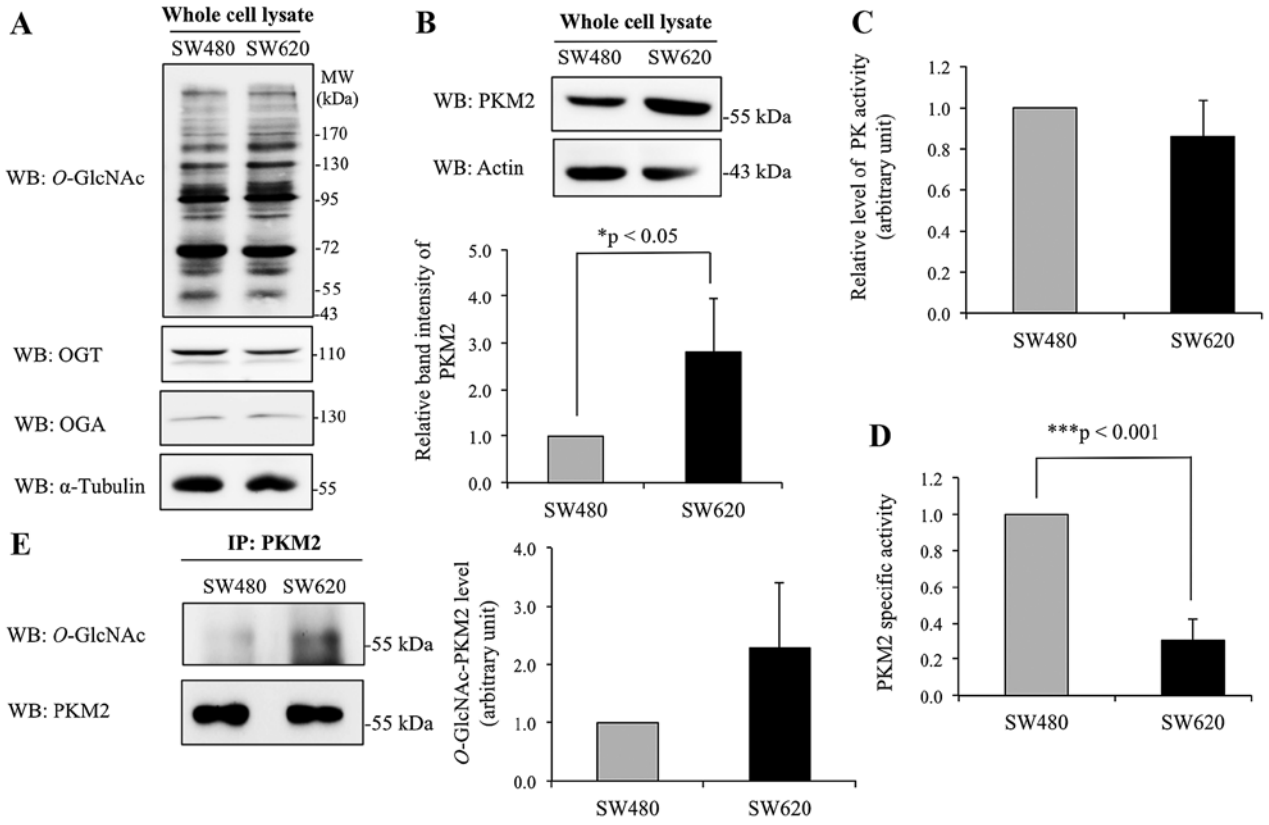

Figure 5. *O*-GlcNAcylation of PKM2 in non-metastatic SW480 and metastatic SW620 cells. (A) Immunoblots of *O*-GlcNAc, OGT, OGA, and α-tubulin in whole cell lysates of SW480 and SW620 cells. (B) Representative immunoblot of PKM2 in whole cell lysates of SW480 and SW620 cells. (C) Relative activity of pyruvate kinase activity in whole cell lysates of SW480 and SW620. (D) PKM2-specific activity in SW480 and SW620 whole cell lysates calculated from relative pyruvate kinase activity (C) normalized to PKM2 expression level detected by immunoblotting (B). (E) Representative immunoblots and relative band intensity of *O*-GlcNAc modified-PKM2 and total PKM2 immunoprecipitated from SW480 and SW620 cells. Data are presented as means ± SD from three independent experiments. PKM2, pyruvate kinase M2; OGT, *O*-GlcNAc transferase; OGA, *O*-GlcNAcase.

However, basal levels of *O*-GlcNAcylation and its cycling enzymes, OGT and OGA, did not differ between the colorectal cancer cell lines originating from primary (SW480) and metastatic sites (SW620) of the same patient (Fig. 5A). Thus, the role of *O*-GlcNAcylation in modulating complex signaling pathways in cancer still needs to be understood.

Apart from the potential roles of *O*-GlcNAcylation in regulating myriad signaling pathways, crosstalk between *O*-GlcNAcylation and phosphorylation has also emerged as a significant fine-tuning regulatory mechanism in various diseases including diabetes, Alzheimer's and cancer (13). We therefore interfered with the basal level of *O*-GlcNAcylation by knocking down the *OGT* gene or inhibiting OGA activity using the potent inhibitor TMG, and observed the subsequent phosphorylation profiles. The results from 2DE immunoblots indicated that the intensity of serine phosphorylation was significantly decreased in at least 5 protein spots including SHMT, cytokeratin-8, PKM2, HNRNPL and lamin-B1 upon decrease of global *O*-GlcNAcylation (Fig. 2). This observation suggests that the 'Yin-Yang' model, in which the two modifications compete for the same or proximal sites (19), is inadequate. Consistent with our findings, globally increased *O*-GlcNAcylation in NIH-3T3 cells by inhibition of OGA induced an unexpected elevation of phosphorylation at 149 sites (~18% of phosphosites), caused no alteration in ~48% of phosphosites and decreased phosphorylation at 280 sites (~33% of phosphosites) from 1,564 identified proteins (20). Thus, it appears that crosstalk between *O*-GlcNAcylation and phosphorylation is not exclusively antagonistic, but can lead to a synergistic outcome. A possible explanation is that each modification may regulate the cycling enzymes of the other modifications. Indeed, OGT itself is phosphorylated at Tyr979, although a well-defined function of phosphorylation on OGT activity is still awaited (13). Furthermore, *O*-GlcNAcylation has been reported to regulate the activities of some kinases including Ca^{2+}/calmodulin-dependent protein kinase IV (CaMKIV) (21), Akt (22) and PKC (23). Dias *et al* also studied a wide range of kinases and revealed 42 kinases which acted as substrates for OGT (14).

SHMT is a key one-carbon donor required for *de novo* nucleotide biosynthesis and DNA methylation (24,25). Two isoforms of SHMT, SHMT1 and SHMT2, were found as cytosolic and mitochondrial isoforms, respectively. However, only the mitochondrial isoform SHMT2, and not the cytosolic isoform, has a significant impact on cancer cell proliferation (26). Here, we found decreased phosphorylation of SHMT2, when global *O*-GlcNAcylation was decreased (Fig. 2 and Table I). However, there is still no information on the role of serine phosphorylation of SHMT2. According to 2DE immunoblots, SHMT2 is also modified by *O*-GlcNAcylation in HT29 cells. Since SHMT2 is a crucial enzyme in mitochondrial glycine synthesis pathway, further study on regulation of SHMT2 by *O*-GlcNAcylation would be of interest.

Cytokeratin-8 or keratin-8 (CK8) is an intermediate filament protein in epithelial cells and classified as a basic-to-neutral type II keratin (27). Chou *et al* first reported *O*-GlcNAc-modification of CK8 in 1992 (28). Cellular CK8 exists in two forms, which are the soluble and filamentous forms, respectively. Higher *O*-GlcNAcylation in conjunction with enhanced serine phosphorylation of CK8 was notably found in the soluble fraction of immortalized Chang cells and heat stress-induced HepG2 cells (29-31). Our finding of synergistic effect of these two PTMs is therefore inconsistent with previous studies.

HNRNPL is an RNA-binding protein, which exhibits a binding preference for CA-repeat and CA-rich RNA elements (32). HNRNPL has been reported as a substrate for CaMKIV (33). The Ser513 phosphorylated site of HNRNPL is crucial for an interaction of HNRNPL with the CaMKIV-responsive RNA element 1 of stress axis-regulated exon of the *Slo1* mRNA that governs splicing patterns and provides composition of potassium channels. Here, we demonstrated that HNRNPL is potentially *O*-GlcNAc-modified in HT29 cells (Fig. 2 and Table I). Moreover, *O*-GlcNAcylation of many HNRNP family members was reported in cancer tissues, suggesting the role of *O*-GlcNAcylation in tumorigenesis (15).

Lamin-B1 (LB1) is a main nuclear structural protein that has important roles in the regulation of various processes taking place in nucleus including DNA, RNA processes and chromatin remodeling (34). Nuclear PKC catalyzes phosphorylation of LB1, which subsequently induces cell cycle progression through mitosis (35,36). However, we did not observe *O*-GlcNAcylation of LB1 on the 2DE blot from HT29 whole cell lysates. Subcellular enrichment of nuclear fraction may enhance detection (Fig. 2 and Table I).

In HT29 cells, we showed that serine phosphorylation level of PKM2 was modulated owing to changes of global *O*-GlcNAcylation level (Fig. 3A and B). We also examined the effect of *O*-GlcNAcylation on pyruvate kinase activity. The results showed that PK activity of PKM2 was decreased when *O*-GlcNAcylation was increased by inhibiting OGA enzyme (Fig. 4). This is consistent with a study from Yi *et al* that PK activity was modestly decreased in PUGNAc-treated and OGT-overexpressing 293T cells (37). Furthermore, OGT knockdown in HT29 cells also caused a significantly higher PKM2-specific activity. In SW620 cells, higher *O*-GlcNAcylation of PKM2 was observed, in conjunction with lower PKM2-specific activity, when compared to SW480 cells (Fig. 5). As shown in Fig. 3C, the predicted *O*-GlcNAc-modification sites are located in various regions throughout the PKM2 structure, so regulation of PK activity by interfering with the tetramer to dimer ratio or blocking allosteric regulation may occur (38,39). PKM2 may be modified by various PTMs, including phosphorylation, acetylation and oxidation as shown in Fig. 3C, which may regulate its catalytic activity.

Furthermore, one of the most striking observations of this study is the role of *O*-GlcNAcylation in regulating PKM2 expression, both at mRNA and protein levels (Fig. 4). The expression of PKM2 was modulated in consonance with levels of *O*-GlcNAcylation. Interestingly, it has been previously reported that overexpression of hepatic forkhead box O1 (FoxO1) decreased an expression level of liver pyruvate kinase (PKL) through suppression *O*-GlcNAcylation of carbohydrate response element binding protein (Chrebp) (40). *O*-GlcNAcylation stabilized Chrebp by inhibiting ubiquitination that enhanced the recruitment of Chrebp to PKL promoter. PKM2 expression is also regulated by SP1 transcription factor (41). In high glucose environment, dephosphorylation of SP1 induces binding of SP1, thus increasing PKM2 expression level (41). Interestingly, Jackson and Tjian reported *O*-GlcNAcylation of SP1 (42). Moreover, reciprocal interplay between *O*-GlcNAcylation and phosphorylation of SP1 was observed in HT29 cells as PUGNAc-treated HT29 cells exhibited a reduction of phosphorylation on SP1 (43). It is likely that elevated *O*-GlcNAcylation enhances binding activity of SP1 to PKM2 promoter leading to upregulation of PKM2 expression. Therefore, understanding the mechanism of *O*-GlcNAcylation in regulating PK activity and the expression profile of PKM2 is still a challenge.

In conclusion, we have explored the interplay of *O*-GlcNAcylation and serine phosphorylation by knocking down *OGT* gene in colorectal cancer cell lines. Decreasing *O*-GlcNAc levels led to a reduction of serine phosphorylation of many proteins. Using the combination of 2DE *O*-GlcNAc and phospho-immunoblotting, followed by LC-MS/MS analysis, we found that PKM2 was modified by *O*-GlcNAc and phospho-serine. Importantly, an alteration of global *O*-GlcNAcylation affected levels of serine-phosphorylation on PKM2 that may relate to kinase activity of PKM2. Here, we demonstrated that lower global *O*-GlcNAcylation led to decreased PKM2 expression, but induced a higher PKM2-specific activity, while increasing *O*-GlcNAcylation by TMG treatment had the opposite result. In addition, the metastatic colorectal cancer SW620 cells were found to have more *O*-GlcNAc-PKM2 and exhibited lower PKM2-specific activity in comparison to the non-metastatic colorectal cancer SW480 cells. Taken together, these data suggest that *O*-GlcNAcylation of PKM2, at least in part, controls PKM2 activity and expression, thereby regulating the glycolytic pathway to facilitate the Warburg effect that is beneficial for bioenergetics and biosynthesis of cancer cells.

Acknowledgements

This study was supported by the Chulabhorn Research Institute (CRI), the Chulabhorn Graduate Institute (CGI), and the Center of Excellence on Environmental Health and Toxicology (EHT).

References

1. Wong N, Ojo D, Yan J and Tang D: PKM2 contributes to cancer metabolism. Cancer Lett 356: 184-191, 2015.
2. Tamada M, Suematsu M and Saya H: Pyruvate kinase M2: Multiple faces for conferring benefits on cancer cells. Clin Cancer Res 18: 5554-5561, 2012.
3. Vander Heiden MG, Cantley LC and Thompson CB: Understanding the Warburg effect: The metabolic requirements of cell proliferation. Science 324: 1029-1033, 2009.
4. Christofk HR, Vander Heiden MG, Harris MH, Ramanathan A, Gerszten RE, Wei R, Fleming MD, Schreiber SL and Cantley LC: The M2 splice isoform of pyruvate kinase is important for cancer metabolism and tumour growth. Nature 452: 230-233, 2008.
5. Yang W and Lu Z: Regulation and function of pyruvate kinase M2 in cancer. Cancer Lett 339: 153-158, 2013.

6. Mazurek S, Boschek CB, Hugo F and Eigenbrodt E: Pyruvate kinase type M2 and its role in tumor growth and spreading. Semin Cancer Biol 15: 300-308, 2005.
7. Hanover JA, Krause MW and Love DC: The hexosamine signaling pathway: O-GlcNAc cycling in feast or famine. Biochim Biophys Acta 1800: 80-95, 2010.
8. Lazarus MB, Nam Y, Jiang J, Sliz P and Walker S: Structure of human O-GlcNAc transferase and its complex with a peptide substrate. Nature 469: 564-567, 2011.
9. Chaiyawat P, Netsirisawan P, Svasti J and Champattanachai V: Aberrant O-GlcNAcylated proteins: New perspectives in breast and colorectal cancer. Front Endocrinol (Lausanne) 5: 193, 2014.
10. Willems L, Jacque N, Jacquel A, Neveux N, Maciel TT, Lambert M, Schmitt A, Poulain L, Green AS, Uzunov M, *et al*: Inhibiting glutamine uptake represents an attractive new strategy for treating acute myeloid leukemia. Blood 122: 3521-3532, 2013.
11. Mi W, Gu Y, Han C, Liu H, Fan Q, Zhang X, Cong Q and Yu W: O-GlcNAcylation is a novel regulator of lung and colon cancer malignancy. Biochim Biophys Acta 1812: 514-519, 2011.
12. PhueaouanT,ChaiyawatP,NetsirisawanP,ChokchaichamnankitD, Punyarit P, Srisomsap C, Svasti J and Champattanachai V: Aberrant O-GlcNAc-modified proteins expressed in primary colorectal cancer. Oncol Rep 30: 2929-2936, 2013.
13. Butkinaree C, Park K and Hart GW: O-linked beta-N-acetylglucosamine (O-GlcNAc): Extensive crosstalk with phosphorylation to regulate signaling and transcription in response to nutrients and stress. Biochim Biophys Acta 1800: 96-106, 2010.
14. Dias WB, Cheung WD and Hart GW: O-GlcNAcylation of kinases. Biochem Biophys Res Commun 422: 224-228, 2012.
15. Champattanachai V, Netsirisawan P, Chaiyawat P, Phueaouan T, Charoenwattanasatien R, Chokchaichamnankit D, Punyarit P, Srisomsap C and Svasti J: Proteomic analysis and abrogated expression of O-GlcNAcylated proteins associated with primary breast cancer. Proteomics 13: 2088-2099, 2013.
16. Srisomsap C, Sawangareetrakul P, Subhasitanont P, Panichakul T, Keeratichamroen S, Lirdprapamongkol K, Chokchaichamnankit D, Sirisinha S and Svasti J: Proteomic analysis of cholangiocarcinoma cell line. Proteomics 4: 1135-1144, 2004.
17. Tit-Oon P, Chokchaichamnankit D, Khongmanee A, Sawangareetrakul P, Svasti J and Srisomsap C: Comparative secretome analysis of cholangiocarcinoma cell line in three-dimensional culture. Int J Oncol 45: 2108-2116, 2014.
18. Livak KJ and Schmittgen TD: Analysis of relative gene expression data using real-time quantitative PCR and the 2(-Delta Delta C(T)) method. Methods 25: 402-408, 2001.
19. Hu P, Shimoji S and Hart GW: Site-specific interplay between O-GlcNAcylation and phosphorylation in cellular regulation. FEBS Lett 584: 2526-2538, 2010.
20. Wang Z, Gucek M and Hart GW: Cross-talk between GlcNAcylation and phosphorylation: Site-specific phosphorylation dynamics in response to globally elevated O-GlcNAc. Proc Natl Acad Sci USA 105: 13793-13798, 2008.
21. Dias WB, Cheung WD, Wang Z and Hart GW: Regulation of calcium/calmodulin-dependent kinase IV by O-GlcNAc modification. J Biol Chem 284: 21327-21337, 2009.
22. Luo B, Soesanto Y and McClain DA: Protein modification by O-linked GlcNAc reduces angiogenesis by inhibiting Akt activity in endothelial cells. Arterioscler Thromb Vasc Biol 28: 651-657, 2008.
23. Robles-Flores M, Meléndez L, García W, Mendoza-Hernández G, Lam TT, Castañeda-Patlán C and González-Aguilar H: Post-translational modifications on protein kinase c isozymes. Effects of epinephrine and phorbol esters. Biochim Biophys Acta 1783: 695-712, 2008.
24. Renwick SB, Snell K and Baumann U: The crystal structure of human cytosolic serine hydroxymethyltransferase: A target for cancer chemotherapy. Structure 6: 1105-1116, 1998.
25. Amelio I, Cutruzzolá F, Antonov A, Agostini M and Melino G: Serine and glycine metabolism in cancer. Trends Biochem Sci 39: 191-198, 2014.
26. Jain M, Nilsson R, Sharma S, Madhusudhan N, Kitami T, Souza AL, Kafri R, Kirschner MW, Clish CB and Mootha VK: Metabolite profiling identifies a key role for glycine in rapid cancer cell proliferation. Science 336: 1040-1044, 2012.
27. Schweizer J, Bowden PE, Coulombe PA, Langbein L, Lane EB, Magin TM, Maltais L, Omary MB, Parry DA, Rogers MA, *et al*: New consensus nomenclature for mammalian keratins. J Cell Biol 174: 169-174, 2006.
28. Chou CF, Smith AJ and Omary MB: Characterization and dynamics of O-linked glycosylation of human cytokeratin 8 and 18. J Biol Chem 267: 3901-3906, 1992.
29. Owens DW and Lane EB: The quest for the function of simple epithelial keratins. Bioessays 25: 748-758, 2003.
30. Omary MB, Ku NO, Liao J and Price D: Keratin modifications and solubility properties in epithelial cells and in vitro. Subcell Biochem 31: 105-140, 1998.
31. Srikanth B, Vaidya MM and Kalraiya RD: O-GlcNAcylation determines the solubility, filament organization, and stability of keratins 8 and 18. J Biol Chem 285: 34062-34071, 2010.
32. Rossbach O, Hung LH, Khrameeva E, Schreiner S, König J, Curk T, Zupan B, Ule J, Gelfand MS and Bindereif A: Cross-linking-immunoprecipitation (iCLIP) analysis reveals global regulatory roles of hnRNP L. RNA Biol 11: 146-155, 2014.
33. Liu G, Razanau A, Hai Y, Yu J, Sohail M, Lobo VG, Chu J, Kung SK and Xie J: A conserved serine of heterogeneous nuclear ribonucleoprotein L (hnRNP L) mediates depolarization-regulated alternative splicing of potassium channels. J Biol Chem 287: 22709-22716, 2012.
34. Shimi T, Butin-Israeli V, Adam SA, Hamanaka RB, Goldman AE, Lucas CA, Shumaker DK, Kosak ST, Chandel NS and Goldman RD: The role of nuclear lamin B1 in cell proliferation and senescence. Genes Dev 25: 2579-2593, 2011.
35. Hocevar BA, Burns DJ and Fields AP: Identification of protein kinase C (PKC) phosphorylation sites on human lamin B. Potential role of PKC in nuclear lamina structural dynamics. J Biol Chem 268: 7545-7552, 1993.
36. Fiume R, Ramazzotti G, Teti G, Chiarini F, Faenza I, Mazzotti G, Billi AM and Cocco L: Involvement of nuclear PLCbeta1 in lamin B1 phosphorylation and G2/M cell cycle progression. FASEB J 23: 957-966, 2009.
37. Yi W, Clark PM, Mason DE, Keenan MC, Hill C, Goddard WA III, Peters EC, Driggers EM and Hsieh-Wilson LC: Phosphofructokinase 1 glycosylation regulates cell growth and metabolism. Science 337: 975-980, 2012.
38. Dombrauckas JD, Santarsiero BD and Mesecar AD: Structural basis for tumor pyruvate kinase M2 allosteric regulation and catalysis. Biochemistry 44: 9417-9429, 2005.
39. Mazurek S: Pyruvate kinase type M2: A key regulator of the metabolic budget system in tumor cells. Int J Biochem Cell Biol 43: 969-980, 2011.
40. Ido-Kitamura Y, Sasaki T, Kobayashi M, Kim HJ, Lee YS, Kikuchi O, Yokota-Hashimoto H, Iizuka K, Accili D and Kitamura T: Hepatic FoxO1 integrates glucose utilization and lipid synthesis through regulation of Chrebp O-glycosylation. PLoS One 7: e47231, 2012.
41. Schäfer D, Hamm-Künzelmann B and Brand K: Glucose regulates the promoter activity of aldolase A and pyruvate kinase M2 via dephosphorylation of Sp1. FEBS Lett 417: 325-328, 1997.
42. Jackson SP and Tjian R: O-glycosylation of eukaryotic transcription factors: Implications for mechanisms of transcriptional regulation. Cell 55: 125-133, 1988.
43. Haltiwanger RS, Grove K and Philipsberg GA: Modu-lation of O-linked N-acetylglucosamine levels on nuclear and cytoplasmic proteins in vivo using the peptide O-GlcNAc-beta-N-acetylglucosaminidase inhibitor O-(2-acetamido-2-deoxy-D-glucopyranosylidene)amino-N- phenylcarbamate. J Biol Chem 273: 3611-3617, 1998.